We are IntechOpen,
the world's leading publisher of
Open Access books
Built by scientists, for scientists

4,800
Open access books available

122,000
International authors and editors

135M
Downloads

Our authors are among the

154
Countries delivered to

TOP 1%
most cited scientists

12.2%
Contributors from top 500 universities

CLARIVATE ANALYTICS
BOOK CITATION INDEX
INDEXED

WEB OF SCIENCE™

Selection of our books indexed in the Book Citation Index
in Web of Science™ Core Collection (BKCI)

Interested in publishing with us?
Contact book.department@intechopen.com

Numbers displayed above are based on latest data collected.
For more information visit www.intechopen.com

Automatic Vector Seeded Region Growing for Parenchyma Classification in Brain MRI

Chuin-Mu Wang and Ruey-Maw Chen
National Chin-Yi University of Technology,
Taiwan, R.O.C.

1. Introduction

Nuclear magnetic resonance (NMR) can be used to measure the nuclear spin density, the interactions of the nuclei with their surrounding molecular environment and those between close nuclei, respectively. It produces a sequence of multiple spectral images of tissues with a variety of contrasts using several magnetic resonance parameters. When tissues are classified by means of MRI, the images are multi-spectral. Therefore, if only a single image with a certain spectrum is processed, the goal of tissue classification will not be achieved because the single image can't provide adequate information. Consequently, it is necessary to integrate the information of all the spectral images to classify tissues. Multi-spectral image processing techniques [1-3] are hence employed to collect spectral information for classification and of clinically critical values. In this paper, a new classification approach was proposed, it is called unsupervised Vector Seeded Region Growing (UVSRG). The UVSRG mainly select seed pixel vectors by means of standard deviation and relative Euclidean distance. Through the UVSRG processing, the data dimensionality of MRI can be decreased and the desired target of interest can be classified which the brain tissue and brain tumor segmentation. A series of experiments are conducted and compared to the commonly used c-means method for performance evaluation. The results show that the proposed approach is a promising and effective technique for MR image classification.

Nuclear magnetic resonance (NMR) has recently developed as a versatile technique in many fields such as chemistry, physics, engineering because its signals provide rich information about material structures that involve the nature of a population of atoms, the structure of their environment, and the way in which the atoms interact with environment1. When NMR is applied to human anatomy, NMR signals can be used to measure the nuclear spin density, the interactions of the nuclei with their surrounding molecular environment and those between close nuclei, respectively. It produces a sequence of multiple spectral images of tissues with a variety of contrasts using three magnetic resonance parameters, spin-lattice (T1), spin-spin (T2) and dual echo-echo proton density (PD). By appropriately choosing pulse sequence parameters, echo time (TE) and repetition time (TR) a sequence of images of

specific anatomic area can be generated by pixel intensities that represent characteristics of different types of tissues throughout the sequence. As a result, magnetic resonance imaging (MRI) becomes a more useful image modality than X-ray computerized tomography (X-CT) when it comes to analysis of soft tissues and organs since the information about T1 and T2 offers a more precise picture of tissue functionality than that produced by X-CT2.

MRI shares many image structures and characteristics with remotely sensed imagery. They are acquired as image sequences by spectral channels at different specific wavelengths remotely. Most importantly, they produce a sequence of images which explore the spectral properties and correlation within the sequence so as to improve image analysis. One unique feature for which both multispectral MR images and remote sensing images are in common is spectral properties contained in an image pixel that are generally not explored in classical image processing. Since various material substances can be uncovered by different wavelengths, an MR or remote sensing image pixel is actually a pixel vector, of which each component represents an image pixel acquired by a specific spectral band. There are mainly four types of segmentation techniques, namely global thresholding, boundary-based segmentation, region-based segmentation, and mixed segmentation. Seeded Region Growing is an integrated method brought up by Adams and Bischof [4-13], in which few initial seeds are generated, and more similar neighboring regions are then combined to achieve region growing [14-21]. In addition, the method of unsupervised vector seeded region growing suitable for medical multi-spectral images was established. Vector seed selection mainly selects seed pixel vectors by means of standard deviation and relative Euclidean distance. Seeds emerge from even and smooth regions, so the smaller the standard deviation is, the more concentrated the data distribution is. In terms of image, it indicates that the difference between a pixel vector and the eight neighbors is smaller, and the pixel vector is suitable for the seed pixel vector. Furthermore, relative Euclidean distance is employed to more carefully select the seed pixel vector to accomplish unsupervised classification.

2. Vector seeded region growing

First of all, the multi-spectral images of a brain section were obtained. There wee five images belonging to the same section but different spectrums, respectively Band1, Band2, and Band3. When tissue classification is conducted, the characteristic information of a single image is too insufficient to achieve effects upon tissue classification if only a single image of a particular spectrum is processed. Thus, the images from Band1 to Band3 in order were combined into 3D eigenspace to acquire the 3D eigenvector of every pixel.

Vector seed selection was applied to the aforementioned eigenspace images, or multi-spectral images, to obtain initial seeds. The algorithm of seeded region growing was further adopted to divide the multi-spectral images into many small regions. The algorithm of region merging was employed to merge similar regions as well as to combine smaller regions with the nearest neighboring regions. Finally, all the regions eventually segmented by means of region growing were classified, and the algorithm of K-means clustering was used, in which it was assumed that K=3, to divide the regions into three categories. After the classification was accomplished, the regions in the same category were namely the same type of brain tissues. Figure 1 indicates the algorithmic procedures.
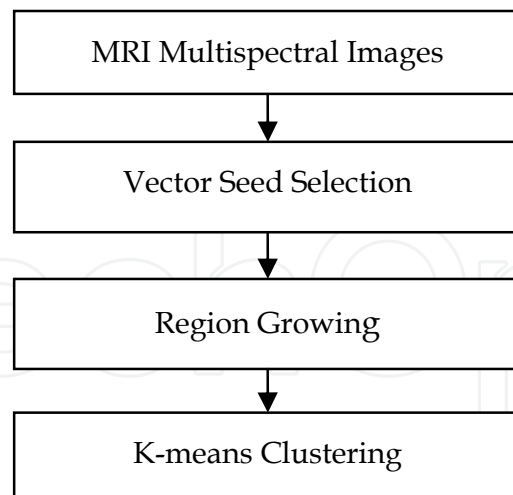
Fig. 1. Algorithmic procedures

2.1 Vector seed selection

Seeded region growing starts from seeds, and each time, it expands around at the speed of one pixel. Hence, a seed point has to be selected in the beginning. In vector seed selection, the pixel vectors which can become seeds have to possess the following characteristics:

a. There should be high similarity between a seed pixel and the neighbors.
b. There should be at least one seed in the expected region.
c. A seed should be unconnected to different regions.

The seed points can be either a single pixel vector or a group of connected pixel vectors, which will be regarded as the same region in region growing. According to the aforesaid characteristics, there are two conditions for each pixel vector in the multi-spectral images to be selected to be a seed point. One is that the similarity between one pixel vector and the eight neighbors should be higher than one threshold. The other one is that the maximum relative Euclidean distance between a seed pixel vector and its eight neighbors should be smaller than a threshold. When the above two conditions are satisfied, a pixel vector becomes a seed point.

Similarity H, the first condition mentioned above, calculated the similarity between each pixel vector, composed of B1~B3, and its eight neighboring points. The standard deviation of pixel vector was calculated by the following equation:

$$\begin{cases} \sigma_{B1} = \sqrt{\dfrac{1}{9}\sum_{i=1}^{9}(B1_i - \overline{B1})^2} \\[2em] \sigma_{B2} = \sqrt{\dfrac{1}{9}\sum_{i=1}^{9}(B2_i - \overline{B2})^2} \\[2em] \sigma_{B3} = \sqrt{\dfrac{1}{9}\sum_{i=1}^{9}(B3_i - \overline{B3})^2} \end{cases} \qquad (1)$$

In the equation, $\overline{B1}$, $\overline{B2}$ and $\overline{B3}$ indicates the mean of the selected 3×3 range, calculated as follows:

$$\begin{cases} \overline{B1} = \dfrac{1}{9}\sum_{i=1}^{9} B1_i \\[2mm] \overline{B2} = \dfrac{1}{9}\sum_{i=1}^{9} B2_i \\[2mm] \overline{B3} = \dfrac{1}{9}\sum_{i=1}^{9} B3_i \end{cases} \tag{2}$$

The overall standard deviation is calculated as follows:

$$\sigma = \sigma_{B1} + \sigma_{B2} + \sigma_{B3} \tag{3}$$

The standard deviation was further normalized by [0, 1] as follows:

$$\sigma_N = \sigma / \sigma_{\max} \tag{4}$$

$\sigma_{\max}$ indicated the maximum standard deviation in the image. The similarity between a pixel vector and its eight neighbors was calculated as follows:

$$H = 1 - \sigma_N \tag{5}$$

Furthermore, according to the second condition, the relative Euclidean distance between each pixel vector and its eight neighboring points was calculated as follows:

$$d_i = \frac{\sqrt{(B1 - B1_i)^2 + (B2 - B2_i)^2 + (B3 - B3_i)^2}}{\sqrt{B1^2 + B2^2 + B3^2}} \tag{6}$$
$$i = 1, 2, \ldots, 8$$

According to the experiment by Shih & Cheng [11], the efficacy of employing relative Euclidean distance is better than that of using normal Euclidean distance. Therefore, the maximum distance between each pixel and its eight neighboring points was calculated by the following equation:

$$d_{\max} = \max_{i=1}^{8}(d_i) \tag{7}$$

The two aforementioned conditions have to be satisfied in order for a pixel vector to be selected as a seed point. The first condition aims at examining whether or not there is considerably high similarity between a seed pixel vector and its neighbors whereas the second condition focuses on ensuring that a seed pixel vector is not in the boundary between two regions.

2.2 Region growing

The traditional method of region growing can not successfully classify brain tissues. Consequently, this paper modified the principle of region growing and recorded all the

pixel vectors connecting with but uncovered by regions. Because the pixel vectors connecting with each other are the priority, these uncovered pixel vectors usually have the judgment upon the distance difference with the connected regions conducted to carry out region growing. It is the major reason why CSF is covered by GM and eroded. Therefore, it is necessary to modify the pixel vector, simultaneously calculate the distance difference with all the regions, and grow it into one of the regions with the minimum difference. The minimum distances were found out from the distances between the pixel vectors and all the regions, each corresponding region with the minimum distance was recorded, and the minimum distances were arranged in the order from small to large in Table T. Due to the order from small to large, the first point 'p' in Table T possessed the minimum difference and the highest similarity with the regions it connected among the pixel vectors in the rims of all the regions. Hence, p is more qualified than all the other uncovered pixel vectors to become a region.

2.3 Applying K-means to region classification

The algorithm of K-means clustering was employed to mainly classify the results of region segmentation in the previous stage. The brain MR images were classified into three categories, respectively GM, WM, and CSF. Because there were many fragmentary regions, it was necessary to classify all the regions, in which all the regions were divided into three categories, it was assumed that K=3, and the region was regarded as a unit to conduct the algorithm of K-means clustering. After the algorithm was accomplished, the regions in the same category belonged to namely the same sort of brain tissue.

3. Experimental results

The real MR images were used for performance evaluation. They were acquired from ten patients with normal physiology. One example is shown in Fig. 2(a)-(e) with the same parameter values in Table 1. Band 1 is the PD-weighted spectral image acquired by the pulse sequence TR/TE = 2500ms/25ms. Bands 2, 3 and 4 are T2-weighted spectral images were acquired by the pulse sequences TR/TE = 2500ms/50ms, TR/TE = 2500ms/75ms and TR/TE =2500ms/100ms respectively. Band 5 is the T1-weighted spectral image acquired by the pulse sequence TR/TE = 500ms/11.9ms. The tissues surrounding the brain such as bone, fat and skin, were semiautomatically extracted using interactive thresholding and masking. The slice thickness of all the MR images are 6mm and axial section were taken from GE MR 1.5T Scanner.

In this experiment, there was one type of real brain MR images. In order to evaluate the performance of the UVSRG, the widely used c-means method (also known as k-means) is used for comparative analysis. The reason to select the c-means method is because it is a spatial-based pattern classification technique. In order to make a fair comparison, the implemented c-means method always designates the desired target signature d as one of its class means with d fixed during iterations.

In order to enhance classification of these MR images, the interfering effects resulting from tissue variability and characterization must be eliminated. However, to identify the sources that cause such interference is nearly impossible unless prior information is provided. On the other hand, in many MRI applications, the three cerebral tissues, GM, WM and CSF are of

major interest where their knowledge can be generally obtained directly from the images. A zero-mean Gaussian noise was added to the phantom images so as to achieve various signal-to-noise ratios (SNR) ranging from 5db to 20db. Table 1 tabulates the values of the parameters used by the MRI pulse sequence and the gray level values of the tissues of each band used as phantom in the experiments and Tables 2-5 tabulate the results for SNR = 20db, 15db, 10 and 5db respectively. In our experiments, the spectral signatures of GM, WM and CSF used for the UVSRG were extracted directly from the MR images. Fig. 3(a)-(c) show the classification results of the UVSRG using five images in Fig. 1(a)-(e). For comparison, we also applied the c-means method to Fig. 2(a)-(e) to produce Fig. 4(a)-(c) where the classification maps of GM, WM and CSF are labeled by (a), (b) and (c) respectively. Compared to Fig. 3(a)-(c), the UVSRG performed significantly better than did the c-means method. All the experimental results presented here were verified by experienced radiologists.

Band #	MRI Parameter	BKG	GM	WM	CSF
Band 1	TR/TE=2500ms/25ms	3	207	188	182
Band 2	TR/TE=2500ms/50ms	3	219	180	253
Band 3	TR/TE=2500ms/75ms	3	150	124	232
Band 4	TR/TE=2500ms/100ms	3	105	94	220
Band 5	TR/TE=500ms/11.9ms	3	95	103	42

Table 1. Gray level values used for the five bands of the test phantom

	N	$N_D(d)$	$N_F(d)$	$R_D(d)$	$R_F(d)$	R_D	R_F
GM	9040	9040	0	1	0		
WM	8745	8745	0	1	0	1	0
CSF	3282	3282	0	1	0		

Table 2. Detection results with SNR = 20 db

	N	$N_D(d)$	$N_F(d)$	$R_D(d)$	$R_F(d)$	R_D	R_F
GM	9040	9040	0	1	0		
WM	8745	8745	0	1	0	1	0
CSF	3282	3282	0	1	0		

Table 3. Detection results with SNR = 15 db

	N	$N_D(d)$	$N_F(d)$	$R_D(d)$	$R_F(d)$	R_D	R_F
GM	9040	9036	8	0.9995	0.0006		
WM	8745	8737	4	0.9990	0.0003	0.9994	0.0004
CSF	3282	3282	0	1	0		

Table 4. Detection results with SNR =10 db

	N	$N_D(d)$	$N_F(d)$	$R_D(d)$	$R_F(d)$	R_D	R_F
GM	9040	8688	455	0.9610	0.0378		
WM	8745	8290	352	0.9479	0.0285	0.9616	0.0280
CSF	3282	3282	0	1	0		

Table 5. Detection results with SNR = 5 db

(a)   (b)   (c)

(d)   (e)
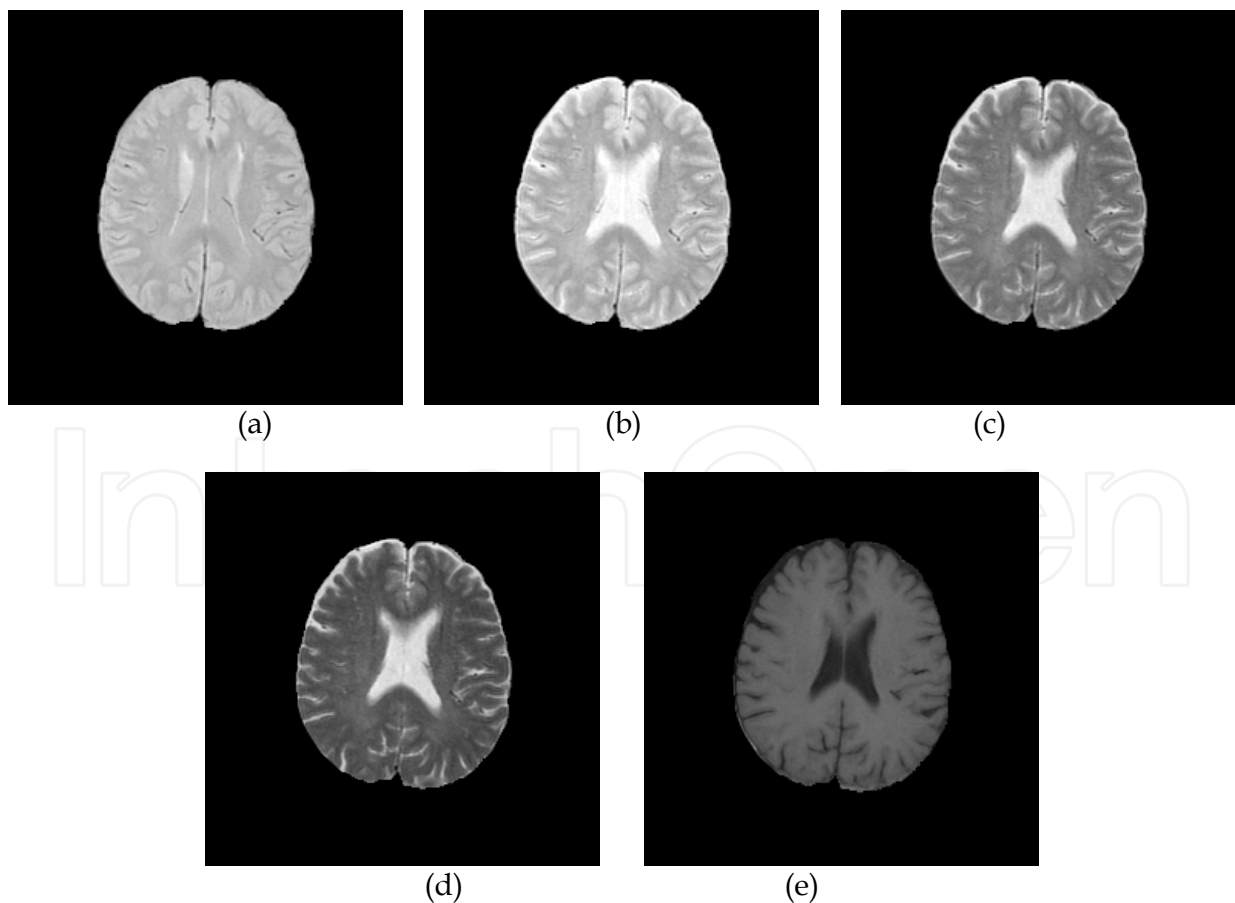
Fig. 2. Real brain MR images. (a) TR1/TE1=2500ms/25ms (b) TR2/TE2=2500ms/50ms (c) TR3/TE3=2500ms/75ms (d) TR4/TE4=2500ms/100ms (e) TR5/TE5=500ms/11.9ms

(a)   (b)   (c)
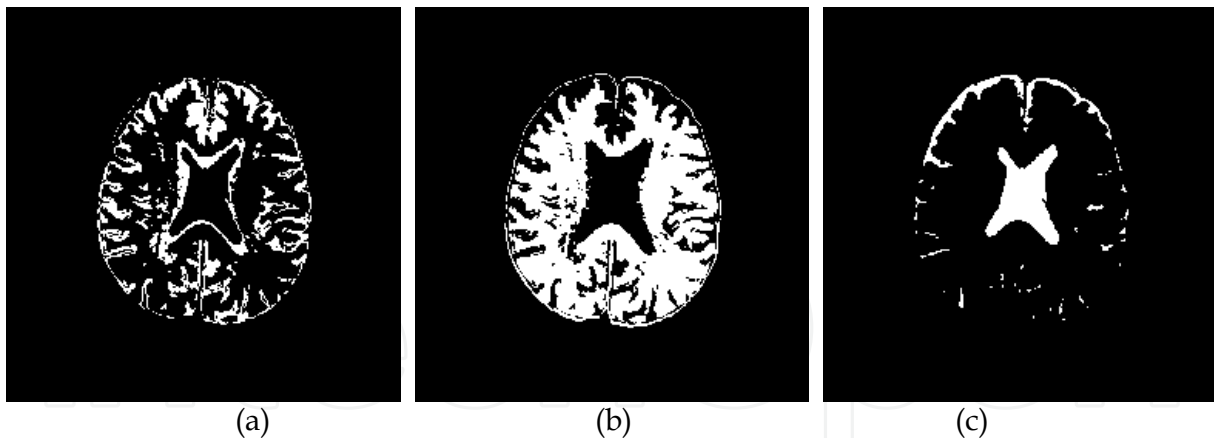
Fig. 3. Real Classification result of brain MR images by UVSRG. (a)GM (b)WM (c)CSF

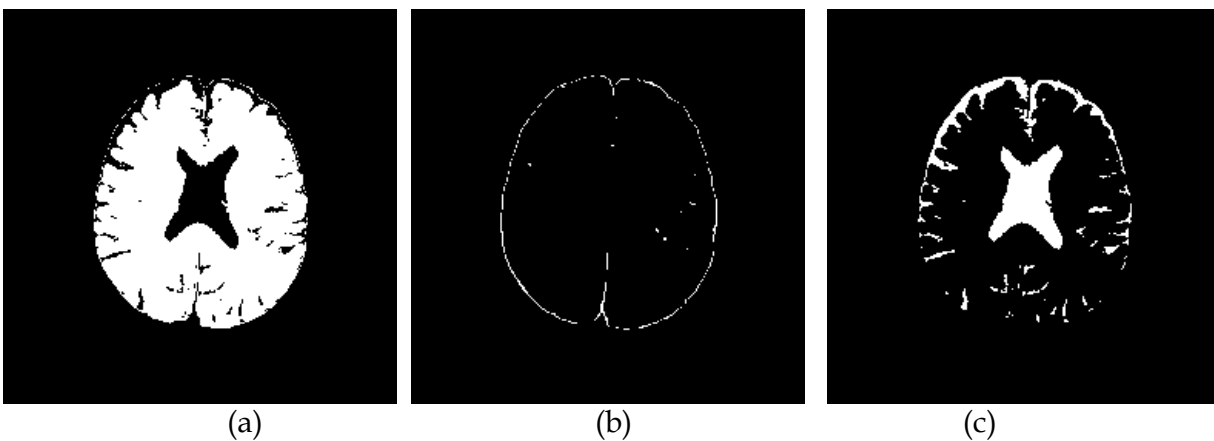(a)   (b)   (c)

Fig. 4. Real Classification result of brain MR images by C-means. (a)GM (b)WM (c)CSF

4. Conclusion

Generally, real brain MR images result from the CSF near the skull, which tends to be close to the boundary in the image. In vector seed selection, seeds tend to appear in more smooth regions. Hence, seeds will not be generated from the pixel vectors in the CSF close to the boundary, which further results in that these tissues are covered by the neighboring gray-scaled tissues in the stage of region growing, and the classification is thus failed. Consequently, this paper improved the method of region growing and successfully applied vector seeded region growing to the classification of brain MR images.

5. References

[1] Di Jia, Fangfang Han, Jinzhu Yang, Yifei Zhang, Dazhe Zhao, Ge Yu, "A Synchronization Algorithm of MRI Denoising and Contrast Enhancement Based on PM-CLAHE Model", JDCTA, Vol. 4, No. 6, pp. 144 ~ 149, 2010

[2] Satish Chandra , Rajesh Bhat , Harinder Singh , D.S.Chauhan , "Detection of Brain Tumors from MRI using Gaussian RBF kernel based Support Vector Machine ", IJACT, Vol. 1, No. 1, pp. 46 ~ 51, 2009

[3] Saif D. Salman & Ahmed A. Bahrani, "Segmentation of tumor tissue in gray medical images using watershed transformation method", IJACT, Vol. 2, No. 4, pp. 123 ~ 127, 2010

[4] J. R. Jimenez-Alaniz, V. Medina-Banuelos, O. Yanez-Suarez, "Data-driven brain MRI segmentation supported on edge confidence and a priori tissue information", IEEE Transactions on Medical Imaging 25 (1) (2006) 74–83.

[5] T. Song, M. M. Jamshidi, R. R. Lee, M. Huang, "A Modified Probabilistic Neural Network for Partial Volume Segmentation in Brain MR Image", IEEE Transactions on Neural Networks 18 (5) (2007) 1424-1432.

[6] J. Tohka, E. Krestyannikov, I. D. Dinov, A. M. Graham, D. W. Shattuck, U. Ruotsalainen, A. W. Toga, "Genetic Algorithms for Finite Mixture Model Based Voxel Classification in Neuroimaging", IEEE Transactions on Medical Imaging 26 (5) (2007) 696-711.

[7] S. Duchesne, A. Caroli, C. Geroldi, C. Barillot, G. B. Frisoni, D. L. Collins, "MRI-Based Automated Computer Classification of Probable AD Versus Normal Controls", IEEE Transactions on Medical Imaging 27 (4) (2008) 509-520.

[8] J. J. Corso, E. Sharon, S. Dube, S. El-Saden, U. Sinha, A. Yuille, "Efficient Multilevel Brain Tumor Segmentation With Integrated Bayesian Model Classification", IEEE Transactions on Medical Imaging 27 (5) (2008) 629-640.

[9] A. Mayer, H. Greenspan, "An Adaptive Mean-Shift Framework for MRI Brain Segmentation", IEEE Transactions on Medical Imaging 28 (8) (2009) 1238-1250.

[10] H. Gudbjartsson, S. Patz, "The Rician distribution of noisy MRI data," Magn. Reson. Med. vol.34, no.6, pp.910–914, 1995.

[11] C. M. Wang, C. C. C. Chen, Y. N. Chung, S. C. Yang, P. C. Chung, C. W. Yang, C. I. Chang, "Detection of Spectral Signatures in Multispectral MR Images for Classification," IEEE Trans. on Medical Imaging, vol.22, no.1, pp.50-61, 2003.

[12] J. R. Jimenez-Alaniz, V. Medina-Banuelos, O. Yanez-Suarez, "Data-driven brain MRI segmentation supported on edge confidence and a priori tissue information," IEEE Trans. on Medical Imaging, vol.25, no.1, pp.74–83, 2006.

[13] R. Adams, L. Bischof, "Seeded region growing," IEEE Trans. on Pattern Analysis and Machine Intelligence, vol.16, no.6, pp.641–647, 1994.

[14] T. Pavlidis, Y.T. Liow, "Integrating region growing and edge detection," IEEE Trans. on Pattern Analysis and Machine Intelligence, vol.12, no.3, pp. 225–233, 1990.

[15] N.R. Pal, S.K. Pal, "A review on image segmentation techniques," Pattern Recognition, vol.26, no.9, pp.1277–1294, 1993.

[16] C. Chu, J.K. Aggarwal, "The integration of image segmentation maps using region and edge information," IEEE Transactions on Pattern Analysis and Machine Intelligence, vol.15, no.2, pp.1241–1252, 1993.

[17] A. Tremeau, N. Bolel, "A region growing and merging algorithm to color segmentation," Pattern Recognition, vol.30, no.7, pp.1191–1203, 1997.

[18] S.A. Hojjatoleslami, J. Kittler, "Region growing: a new approach," IEEE Trans. on Image Processing, vol.7, no.7, pp.1079–1084, 1998.

[19] J. Fan, D.K.Y. Yau, A.K. Elmagarmid, W.G. Aref, "Automatic image segmentation by integrating color-edge extraction and seeded region growing," IEEE Transactions on Image Processing, vol.10, no.10, pp.1454–1466, 2001.

[20] F. Y. Shih, S. Cheng, "Automatic seeded region growing for color image segmentation," Image and Vision Computing, vol.23, no.10, pp.877–886, 2005.

[21] R.O. Duda and P.E. Hart, "Pattern Classification and Scene Analysis," John Wiley and Sons, NY, 1973.
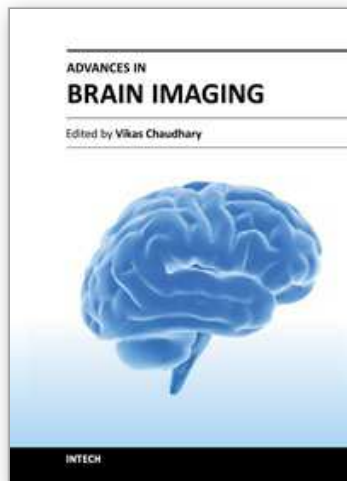
Advances in Brain Imaging

Edited by Dr. Vikas Chaudhary

Remarkable advances in medical diagnostic imaging have been made during the past few decades. The development of new imaging techniques and continuous improvements in the display of digital images have opened new horizons in the study of brain anatomy and pathology. The field of brain imaging has now become a fast-moving, demanding and exciting multidisciplinary activity. I hope that this textbook will be useful to students and clinicians in the field of neuroscience, in understanding the fundamentals of advances in brain imaging.

How to reference

In order to correctly reference this scholarly work, feel free to copy and paste the following:

Chuin-Mu Wang and Ruey-Maw Chen (2012). Automatic Vector Seeded Region Growing for Parenchyma Classification in Brain MRI, Advances in Brain Imaging, Dr. Vikas Chaudhary (Ed.), ISBN: 978-953-307-955-4, InTech, Available from: http://www.intechopen.com/books/advances-in-brain-imaging/automatic-vector-seeded-region-growing-for-parenchyma-classification-in-brain-mri

INTECH
open science | open minds